EXPERIMENTAL WORKS

UDC 577.112;612.115 doi: https://doi.org/10.15407/ubj92.03.033

THE FIBRIN Bβ125-135 SITE IS INVOLVED IN THE LATERAL ASSOCIATION OF PROTOFIBRILS

E. LUGOVSKOI[1], N. PYDIURA[2], Y. MAKOGONENKO[1]✉, L. URVANT[1], P. GRITSENKO[1], I. KOLESNIKOVA[1], N. LUGOVSKA[1], S. KOMISARENKO[1]

[1]Palladin Institute of Biochemistry, National Academy of Sciences of Ukraine, Kyiv;
[2]Institute of Food Biotechnology and Genomics, National Academy of Sciences of Ukraine Kyiv;
✉e-mail: ymakogonenko@gmail.com

Received: 19 May 2020; **Accepted:** 30 June 2020

Earlier we reported that during the human fibrinogen to fibrin transition a neoantigenic determinant was exposed in the Bβ119-133 fragment, where a hinge locus is situated. The fibrin-specific mAb FnI-3c and its Fab-fragment with epitope in this fragment inhibited the lateral association of protofibrils. We suggested that the epitope coincided with a site involved in this process. In this work we investigated the epitope location more precisely and defined a functional role for its exposure in the hinge locus of the molecule. It was found that mAb FnI-3c bound to human, horse and rabbit fibrins, all of which have Lys in the position corresponding to human BβK130, but not to bovine and rat fibrins, which have other amino acid residues in this position, strongly suggesting that BβK130 provides the integral part of the epitope. This fact, homology data, and structural biological analysis of the amino acid sequences around BβK130 indicate that the site of interest is localized within Bβ125-135. The synthetic peptides Bβ121-138 and Bβ125-135, unlike their scrambled versions, bound to mAb FnI-3c in SPR analysis. Both peptides, but not their scrambled versions, inhibited the lateral association of protofibrils. The FnI-3c epitope is exposed after fibrinopeptide A cleavage and desA fibrin monomer formation. Structural biological analysis of the fibrinogen to fibrin transition showed a distinct increase of flexibility in the hinge locus. We propose that the structural transformation in the fibrin hinge regions leads to the conformation necessary for lateral association of protofibrils.

K e y w o r d s: fibrinogen to fibrin transition, coiled-coil connector, protofibril lateral association, hinge region, neoantigenic determinant.

Introduction

Fibrinogen is a dimer, with each subunit of the molecule being formed by three polypeptide chains: Aα, Bβ and γ. The molecule consists of a central E, two peripheral D, and two extended αC regions [1]. The central E-region consisting of (Aα1-104, Bβ1-133, γ1-72)$_2$ is connected to the two peripheral D-regions (Aα105-219, Bβ134-461, γ73-411) by two long flexible coiled-coil connectors (Aα48-161, Bβ79-193, γ23-135). The N-terminal parts of the connectors (Aα48-104, Bβ79-133, γ23-62) belong to the E region and the C-terminal parts (Aα105-161, Bβ134-193, γ63-135) to the D regions. A hinge locus (α99-110, β130-155, γ70-100) is located in the middle part of the coiled-coil region [2, 3]. The extended αC regions (Aα220-610) consist of unfolded flexible segments (Aα220-391) and more structured αC-domains (Aα392-610).

Intermolecular binding of the fibrin polymerization sites A:a as well as putative C:c sites [4], leads to protofibril formation. The protofibrils associate laterally, initially forming fibrils and, subsequently, a three-dimensional fibrin net. At the stage of protofibrils and fibril formation, inter-protofibril binding

of the fibrin polymerization sites B:b increases the rate of protofibril lateral association. While the fibrin protofibril formation mechanism is relatively well-studied, the mechanism of their lateral association remains elusive. It has been suggested that the lateral association is realized by interactions of the DD-regions from neighboring protofibrils [5]. The likely sites of interacting regions were determined by Yang et al. [5] as γ350-360 and γ370-380.

Kollman et al. [6] have observed antiparallel contacts of fibrinogen coiled-coil regions in crystals of human fibrinogen. The authors proposed that fibrin molecules belonging to different protofibrils also interacted by their coiled-coil regions during the lateral association of protofibrils. It is notable that point mutations in the coiled-coil connectors of the fibrinogen molecule lead to impairment of fibrin polymerization, showing the functional significance of this region [7]. Earlier we obtained mAb FnI-3c, an antibody that reacted with human fibrin but not with fibrinogen or the D-dimer, testifying to a structural rearrangement in the epitope during the fibrinogen to fibrin transition. In a preliminary study, the epitope for this mAb in fibrinogen was localized in the coiled-coil region of the molecule Bβ119-133 because the mAb reacted with the fibrin β-chain, but not with the Bβ1-118 and Bβ134-461 fragments of human t-NDSK and D-dimer fragments, respectively. MAb FnI-3c and its corresponding Fab-fragment inhibited the lateral association of fibrin protofibrils. We suggested that this inhibition was the result of blocking the mAb epitope, which coincided with the site involved in the protofibril lateral association [8].

On the basis of primary structural analysis of fibrinogen chains, Doolittle [2] proposed the existence of a hinge region in the coiled-coil region of the fibrinogen molecule. Other authors considered the fragment of the coiled-coil connector consisting of Aα64-114, Bβ100-150, and γ37-87 as a soft hinge about which the molecule adopts different conformations [9]. The crystal structure of human fibrinogen provided experimental evidence of the existence and flexibility of hinge loci [6]. Kohler et al. [3] localized *in silico* the hinge locus in fibrinogen, although the model was lacking residues of βN1-57 and α201-562; they investigated the mechanism and the functional role of the hinge bending motions in fibrin polymerization, fibrinolysis and interaction with the cells. Their results define the hinge locus as including Aα99-110, Bβ130-155 and γ70-100. Other authors assume that flexibility in the hinge allows the Y-ladder single-chain model of protofibrils to be realized, a provision not yet generally accepted.

Taking into consideration the data cited above, as well as our previous data on the inhibition of lateral association by fibrin-specific mAb FnI-3c, we investigated the localization of the mAb FnI-3c epitope at Bβ119-133, including the stage of fibrin polymerization when the epitope exposure takes place, the structure of the hinge itself, and, finally, the functional role of the structural rearrangement in the hinge locus of the coiled-coil region of the fibrin molecule.

Materials and Methods

Tris[hydroxymethyl]aminomethan base, PMSF, aprotinin, HEPES, Tween-20, N-(dimethylaminopropyl)-N′-ethylcarbodiimide hydrochloride, 11-mercaptoundecanoic acid, 6-mercapto-1-hexanol, sodium chloride, urea, guanidine chloride, horse fibrinogen, and sheep anti-mouse IgG-HRP conjugate were obtained from Sigma-Aldrich (St.Louis, Missouri, USA). N-hydroxysuccinimide was obtained from ThermoFisher Scientific (Waltham, MA, USA).

Preparation of fibrinogen, human fibrin, thrombin and plasmin. Human, bovine, rat and rabbit fibrinogens and human desAB fibrin monomer were obtained as described previously [10, 11]. DesA fibrin monomer was prepared with Reptilase or thrombin [12]. Thrombin was obtained from blood plasma in accordance with published procedure [13]. Plasminogen was purified from human plasma using lysine-Sepharose [14]. Plasmin was prepared as previously described [15].

Abbreviations: ELISA – enzyme-linked immunosorbent assay; FpA – fibrinopeptide A; FpB – fibrinopeptide B; GPRP – Gly-Pro-Arg-Pro; HEPES – 2-[4-(2-hydroxyethyl)piperazin-1-yl]ethanesulfonic acid; HF – hydrogen fluoride; HPLC – high performance liquid chromatography; HRP – horseradish peroxidase; mAb – monoclonal antibody; MHBA – Matured Hop Bitter Acids; PAAG – Polyacrylamide Gel; PBS – 0.01 M potassium-phosphate buffer, pH 7.4 with 0.14 M NaCl; PC – principal component; PCA – principal component analysis; PMSF – phenylmethanesulphonyl fluoride; RMSF – root mean square fluctuation; SAS – solvent accessible surface; SDS – sodium dodecyl sulfate; SPPS – solid-phase peptide synthesis; SPR – surface plasmon resonance; t-NDSK – NH_2-terminal disulphide knot of fibrin $(Aα17-51, Bβ15-118, γ1-78)_2$.

Peptide synthesis. Synthetic peptides Bβ121-138 and Bβ109-126 were synthesized by a solid-phase method (Fmoc chemistry) with 96% purity and identified by mass-spectrometry (MALDI) using the Bruker microflex LT (Billerica, Massachusetts, USA).

Scrambled versions of the peptides Bβ121-138 and Bβ125-135 were synthesized by a standard Boc-SPPS procedure on MBHA-modified polystyrol. The products were cleaved from the polymer by anhydrous HF, purified with HPLC and identified by mass-spectrometry (MALDI) using the Bruker microflex LT.

Preparation and purification of mAb. Hybridomas were obtained as described by Köhler and Milstein [16]. Human fibrin desAB in PBS with 2 M urea was used as an antigen. MAb FnI-3c [8] was isolated from hybridoma culture medium by affinity chromatography on protein G-Sepharose 4B (Amersham, Uppsala, Sweden). The determination of immunoglobulin class and subclass was performed by ELISA using the Isotyping kit ("Clinical Credential; ICN Immunobiologicals", Lisle, IL, USA).

Turbidity analysis of fibrin polymerization. The effect of the mAb or its Fab-fragment on fibrin polymerization was studied spectro-photometrically at 350 nm [4, 17]. The curve of increasing turbidity during fibrin polymerization has the following parameters: τ – the lag time representing the time of the protofibril formation; V_{max} – the maximum rate of the fibrin polymerization defined as a tangent of the angle of the turbidity time-dependence at the point of maximum steepness; and h – the maximum turbidity of fibrin clots [4]. The polymerization of desAB fibrins was conducted at 0.1 mg/ml protein in 0.05 M ammonium acetate, pH 7.4, with 0.1 M NaCl and 10^{-4} M $CaCl_2$.

SPR analysis. The exposure of the neoantigenic determinant in fibrin in real time was detected by the SPR method using the Plasmon 6 device, developed in the VE Lashkarev Institute of Semiconductor Physics of the National Academy of Sciences of Ukraine (Kyiv, Ukraine). The gold surface of a chip was covered by the self-assembled layer formed of 11-mercaptoundecanoic acid and 6-mercapto-1-hexanol [18]. MAbs were immobilized covalently onto the functionalized chip using standard amino group coupling chemistry. The fibrin-specific mAb FnI-3c was put into the working cell and the fibrinogen-specific mAb FnII-4d into the control cell. To study an interaction between peptides and mAb FnI-3c, each peptide was introduced into both cells at 0.5 mM concentration in 0.02 M HEPES buffer, pH 7.4, 0.15 M NaCl, and 0.005% Tween-20. The curves presenting the signals from working and control cells and their differences were recorded. To study an interaction *in situ* between fibrin and mAb FnI-3c, the latter was immobilized into working and control cells. Fibrinogen was introduced into the control cell at 1 μg/ml concentration in 0.02 M HEPES buffer, pH 7.4, 0.3 M NaCl, and 0.005% Tween-20. In the working cell, fibrinogen was introduced in the same medium with the addition of 0.001 NIH units/ml of Reptilase. Each curve in the figures represents the typical curve for 2-3 experiments. In the SPR and ELISA experiments, we used human fibrinogen passed through a Sepacryl S-300 was obtained from Sigma-Aldrich (St.Louis, Missouri, USA) for removal of denaturated and aggregated protein molecules that appear in fibrinogen preparations after the thawing procedure.

Electrophoresis and ELISA. SDS electrophoresis in PAAG was performed in accordance with the Laemmli method [19]. The exposure of the neoantigenic determinant during human, horse, bovine, rabbit and rat fibrinogen transformation into fibrin was determined by ELISA. Fibrinogen was added at the concentration of 0.2 mg/ml to the medium, containing 0.02 M HEPES buffer, pH 7.4, and 0.3 M NaCl. The reaction was initiated by thrombin or Reptilase at 0.005 NIH units/ml. At a given time, the reaction was stopped by adding PMSF and aprotinin to final concentrations of 1 mM and 10 μg/ml respectively. Aliquots were withdrawn for electrophoretic and ELISA analysis. Aliquots for ELISA were placed into microtiter plate wells. Neoantigenic determinant exposure was analyzed with mAb FnI-3c as the primary- and sheep anti-mouse IgG-HRP conjugate as the secondary antibodies.

Lysis of fibrinogen and fibrin by plasmin. Lysis of fibrinogen and fibrin by plasmin was performed as previously described at a protein to plasmin molar ratio of 1000:1. The plasmin activity was 15 caseinolytic units per mg of the protein [15].

Bioinformatics analysis. Data on fibrinogen mutations were collected with the help of the GEHT fibrinogen variants database [7] and additional literature searching. Homology models of the human fragments X of fibrinogen and fibrin were constructed using the crystallographic model, Protein Data Bank ID (PDB ID): 3GHG [6], as a template. Model 3GHG contains no coordinates for the unstructured

fragments Bβ1-57, Aα1-26, and Aα213-610 region and thus closely coincides with the structure of the fibrin(ogen) fragment X2 which lacks the residues Bβ1-53 and Aα221-610 [20]. The structure of the FpA (Aα1-16) and residues Aα17-26 were modeled *de novo* and optimized using Modeller9v10 software (Ben Webb, San Francisco, CA 94143, USA) [21-24]. The all-atom contacts model and the geometry evaluation were done with MolProbity (Duke, US) [25]. The dynamical properties of the fragments X of fibrinogen and fibrin were further analyzed by conformational analysis using the package CONCOORD 2.1 (Max Planck Institute for Biophysical Chemistry, Göttingen, Germany) [26]. Ensembles of 100 conformations were obtained for fibrinogen fragment X and fibrin fragment X. Principal component analysis (PCA) was performed using ProDy with NmWiz plugin [27] for VMD (University of Illinois at Urbana-Champaign, Urbana and Champaign, Illinois, USA) [28]. Solvent accessible surface (SAS) area calculations and the preparation of illustrations were carried out in PyMol (Schrodinger, New York, USA) [29]. For fast and sensitive detecting rigid blocks in large macromolecular complexes used method RigidFinder (Yale University, New Haven, Connecticut, USA) [30]. For finge prediction by network analysis of individual protein structures we used StoneHinge (Yale University, New Haven, Connecticut, USA) [31].

Statistical analysis was performed using standard Excel software (Microsoft, Redmond, USA). Mean values and their standard deviations were calculated.

Results and Discussion

Inhibition of protofibril lateral association by synthetic peptides. In order to obtain direct evidence that the epitope of mAb FnI-3c is located in Bβ119-133 and coincides with the site involved in the lateral association of protofibrils, we synthesized three peptides corresponding to amino acid sequences Bβ109-126 (QTSSSSQFVMVLLKDLWQ), Bβ121-138 (LKDLWQKRQKQVKDNENV) and a scrambled version of Bβ121-138 (DKWVQVELKKQKRNDLNQ).

The synthetic peptide Bβ121-138, as opposed to its scrambled version, reacted with mAb FnI-3c in SPR analyses (Fig. 1), confirming the localization of the mAb epitope in this fragment. The Bβ121-138 peptide also inhibited the lateral association of fibrin protofibrils. Based on the results of turbidity analysis

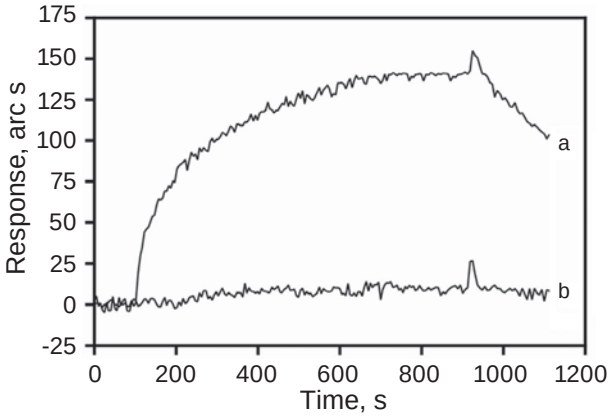

Fig. 1. Binding of synthetic peptide Bβ121-138 and its scrambled version to mAb FnI-3c as detected by the SPR method. Fibrin-specific mAb FnI-3c was immobilized into the working cell and fibrinogen-specific mAb FnII-4d into the control cell of a biosensor chamber. Each peptide was introduced into cells at 0.5 mM concentration in 0.02 M HEPES buffer, pH 7.4, 0.15 M NaCl, with 0.005% Tween-20. The curves of the difference between signals from working and control cells are presented: curve ***a*** *denotes synthetic peptide Bβ121-138 and curve* ***b*** *its scrambled version. Each curve is an average of 2 repeats*

(Fig. 2), we calculated the parameters of the polymerization process: V_{max}, τ and Δh. The peptide at a concentration of 2.5×10^{-4} M caused a 6-fold decrease of the protofibril lateral association rate (V_{max}), increased the lag time (τ) by 2.5 times, and decreased the final clot turbidity (Δh) by 1.4 times. In contrast, the scrambled versions of peptide Bβ121-138 (Fig. 2) and peptide Bβ109-126 (data not shown) did not inhibit fibrin polymerization, testifying to the specific inhibitory activity of peptide Bβ121-138.

The preferential inhibition of the lateral association of protofibrils by mAb FnI-3c, its Fab-fragment, and the peptide Bβ121-138 suggests this site is involved in the process of fibrin protofibril lateral association. Further localization of the FnI-3c epitope in the Bβ121-138 site was based on the observation that the peptide Bβ109-126 did not inhibit fibrin protofibril lateral association, indicating that residues Bβ127-138 must contain the epitope of mAb FnI-3c. To test this hypothesis, we studied the binding of FnI-3c mAb to fibrins of mammalian species that differ in sequence in this region: horse, rabbit, bovine, and rat. FnI-3c bound to human, horse and rabbit fibrins, but not to bovine and rat (Fig. 3, *A*). An alignment of the amino acid sequences shows

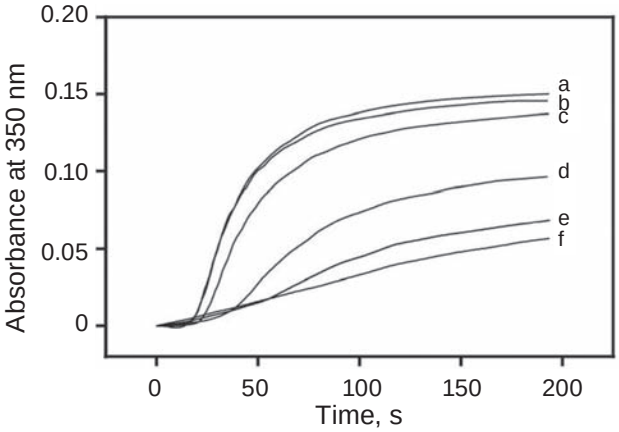

Fig. 2. Turbidity analysis of the inhibition of fibrin desAB polymerization by the synthetic peptide Bβ121-138 and its scrambled version. Curves: ***a****, fibrin desAB polymerization (100 μg/ml) without peptides,* ***b****, fibrin desAB polymerization with scrambled peptide (0.5 mM), fibrin desAB polymerization with* ***c****, 0.125 mM peptide,* ***d****, 0.25 mM peptide,* ***e****, 0.375 mM peptide, and* ***f****, 0.5 mM peptide. Each curve is an average of 2 repeats*

that residue BβK130 is always presents in the Bβ127-138 site in fibrins that bind to mAb FnI-3c (Fig. 3, *B*) but is substituted in bovine and rat fibrins by N and A, respectively, fibrins that do not bind to mAb FnI-3c (Fig. 3, *A*). This fact and the nature of the amino acid sequences around BβK130 indicates that the site of interest is localized within Bβ125-138 of human fibrin.

Taking into consideration that BβLys130 is an integral part of the fibrin-specific mAb FnI-3c epitope, together with analysis of the crystallographic structure of this locus [6], we concluded that the epitope is formed by exposing residues Bβ125-135: Bβ W125 Q126, K127, R128, K130, Q131, K133, D134, and N135 (Fig. 3, *B, C*) during the conversion of fibrinogen to fibrin. To verify this possibility, we synthesized an undecapeptide corresponding to fibrinogen Bβ125-135 (WQKRQKQVKDN) and analyzed its binding to mAb FnI-3c as well as its influence on fibrin polymerization. The peptide bound to mAb FnI-3c (Fig. 4), supporting the localization of the epitope in the Bβ125-135 site. The Bβ125-135 peptide at a concentration of 2.5×10^{-4} M caused a 2-fold decrease of the protofibril lateral association rate (Fig. 5). The scrambled version of Bβ125-135 did not bind to FnI-3c (Fig. 4) and did not inhibit fibrin polymerization (Fig. 5). The Bβ125-135 peptide did not affect the lag time (τ) and decreased the final clot turbidity (Δh) by 1.4 times. Probably, Bβ125-135 is the site where the structural rearrangement takes place during the transformation of fibrinogen to fibrin, which is to say the formation of the epitope of mAb FnI-3c occurs simultaneously with the lateral association of protofibrils.

Structural rearrangements in Bβ125-135 of the monomeric fibrin desA. The question arises, exactly which step of fibrin polymerization involves the structural rearrangement that forms the epitope in Bβ125-135? It seemed possible that the Bβ125-135 site is shielded by the αC region in native fibrinogen, and that the Bβ125-135 site becomes exposed after dissociation of the αC region from the bulk of the molecule. However, in ELISA experiments we did not observe FnI-3c epitope exposure during the hydrolysis of fibrinogen by plasmin, which in the initial step of digestion cleaves αC regions from the molecule (Fig. 6, *A, B*). This indicates that the removal of the αC region from the bulk of the molecule does not lead to the exposure of epitope during fibrinogen to fibrin transformation. In contrast, the results presented in Fig. 6*C* and 6*D* show that the slow cleavage of FpA from fibrinogen by small concentrations of thrombin (0.005 NIH units/ml) at the ionic strength 0.3 correlates with a gradual increase of FnI-3c binding to fibrin desA immobilized on wells of the microplate [11]. Tests with Reptilase produced the same results (data not shown). This clearly indicates that the epitope exposure correlates with FpA cleavage and the conversion of fibrinogen to fibrin desA.

Does the exposure of the epitope take place at the level of the fibrin monomer, or require fibrin oligomer formation when the interactions of the A knob and a hole are realized? To answer this question, we used a molecular system containing fibrinogen (5 mkg/ml) and Reptilase (0.001 NIH units/ml) in 0.02 M HEPES, pH 7.4, 0.3 M NaCl, 0.005% Tween-20, in the absence or presence of 1 mM GPRP peptide. The latter inhibits fibrin polymerization, keeping fibrin in solution. SPR analysis (Fig. 7) did not show any significant difference in the binding of fibrin desA formed *in situ* to mAb FnI-3c immobilized on the chip in the absence or presence of GPRP peptide. Hence, exposure of the epitope and the site involved in the lateral association of protofibrils must be in Bβ125-135 of the fibrin coiled-coil connector at the stage of the fibrin desA monomer formation.

In silico comparison of conformational changes in the hinge loci of the fibrinogen and fibrin frag-

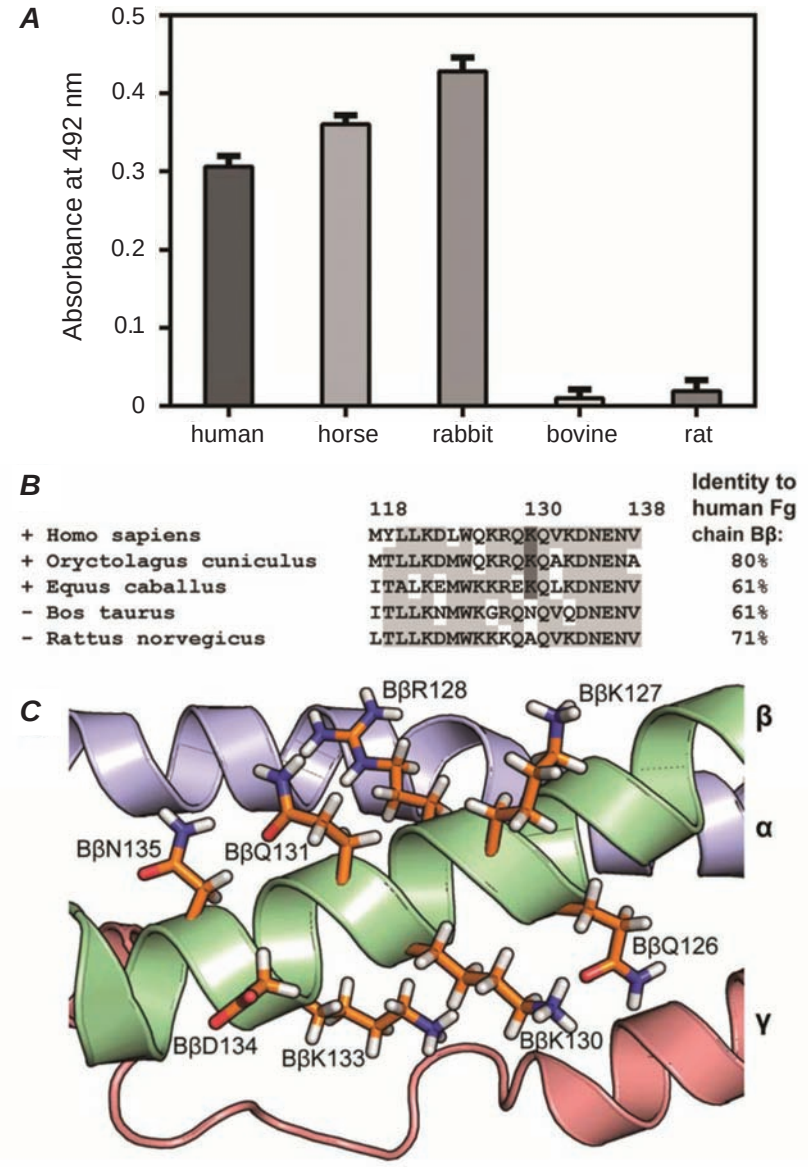

*Fig. 3. Binding of mAb FnI-3c to human and animal fibrins as detected by ELISA. (**A**) Binding of mAb FnI-3c with human, horse, rabbit, bovine, and rat fibrins immobilized in microtiter plate wells. (**B**) Alignment of fragments of human, rabbit, horse, bovine, and rat fibrin(ogen) sequences homologous to the Bβ118-138 fragment of human fibrin(ogen). The percent identity with the human sequence is shown. Identical residues are shown with grey background. The sequences for fibrin(ogen)s binding and non-binding to mAb FnI-3c are marked with "+" or "-" respectively. (**C**) Cartoon of coiled-coil region corresponding to Bβ118-138 based on the crystallographic model of human fibrinogen (PDB ID: 3GHG). The side chains of Bβ chain residues postulated to form the epitope are shown in stick form. Data represent 3 independent experiments. Error bars represent the standard deviations*

ments X. An investigation of the mechanism of conformational changes in the region Bβ125-135 was performed by modeling human fibrinogen and fibrin fragments X. To this end we used the CONCOORD package to obtain ensembles of the two conformations (100 conformations each) and compared their structural properties. We used PCA to specify the localization and the conformational properties of the hinge region, assuming that the hinge would be identified by an extremum on a plot of RMSF of C-alpha atoms. The RMSF of C-alpha atoms of the 20 slowest modes identified the principal com-

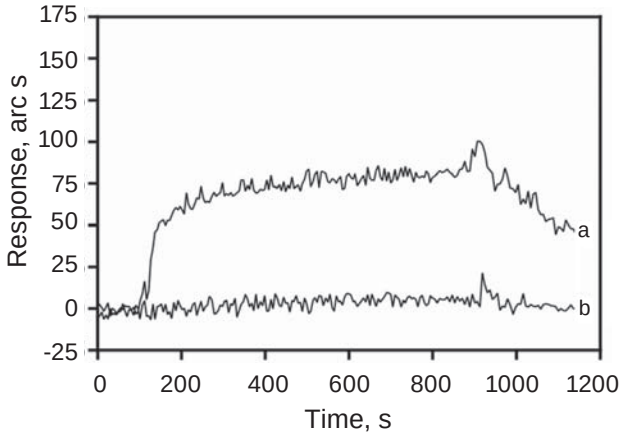

Fig. 4. Binding of synthetic peptides Bβ125-135 and its scrambled version to mAb FnI-3c as detected by the SPR method. Fibrin-specific MAb FnI-3c was immobilized into the working cell and fibrinogen-specific mAb FnII-4d into the control cell of a biosensor chamber. Each peptide was introduced into cells at 0.5 mM concentration in 0.02 M HEPES buffer, pH 7.4, 0.15 M NaCl, with 0.005% Tween-20. The curves of the difference between signals from working and control cells are presented: curve ***a*** *denotes synthetic peptide Bβ125-135 and curve* ***b*** *its scrambled version. Each curve is typical for 3 similar experiments*

ponent 7 (PC7) from the fibrinogen ensemble and PC6 from the fibrin ensemble as the slowest modes describing the hinge movement in the Bβ115-150 sector of the coiled-coil domain in one of the halves of the dimeric fibrin(ogen) molecule. Fig. 8,*A* shows that in these cases the hinge corresponds to a minimum on the RMSF of the C-alpha atoms coinciding with the residues Bβ125-135 in both fibrinogen and fibrin molecules. The correlation coefficient of the values of RMSF of the C-alpha atoms of the fragment Bβ115-150 for these two modes is 0.94. Our PCA data on the ensembles of the fibrin(ogen) conformations and the RigidFinder and StoneHinge web-server predictions allowed us to precisely identify the hinge region location in the fragment of the fibrin(ogen) coiled-coil connector comprising Aα91-103, Bβ125-135, and γ69-77.

The RMSF data showed that the fluctuations of the C-alpha atoms on both sides of the hinge axis are higher for fibrin conformations compared to fibrinogen ones (Fig. 8, *A*), testifying to higher flexibility of the hinge region in fibrin compared to fibrinogen. This finding shows an essential increase of molecular flexibility in the coiled-coil connector in the fibrin molecule after its formation from fibrinogen.

The monoclonal antibody designated mAb FnI-3c reacts with fibrin in its monomer, oligomer and polymer forms, but not with fibrinogen [8]. This means that the transformation of fibrinogen to fibrin leads to the exposure of a stable neoantigenic determinant that retains its structure during the polymerization process. The structural rearrangement leading to neoantigenic determinant formation was found to involve residues Bβ125-135, a region thought to contain a hinge locus for the fibrin molecule.

To identify the possible mechanisms of the neoantigenic determinant exposure during the fibrinogen to fibrin transformation, we performed a comparative conformational analysis of the region Bβ125-135 in models of the fragments X of fibrinogen and fibrin. The per-residue SAS area of the fragment Bβ125-135 was analyzed and models with the lowest and highest areas were selected from ensembles of fibrinogen and fibrin fragments X, respectively (Fig. 8, *B, C, D*). This structural analysis showed (Table) that the amino acid residues Bβ D134 and N135 in the α-helix fragment Bβ125-135 are shielded by a nearby part of the α-helix formed by Bβ N137, V138, V139 in fibrinogen, and that they became

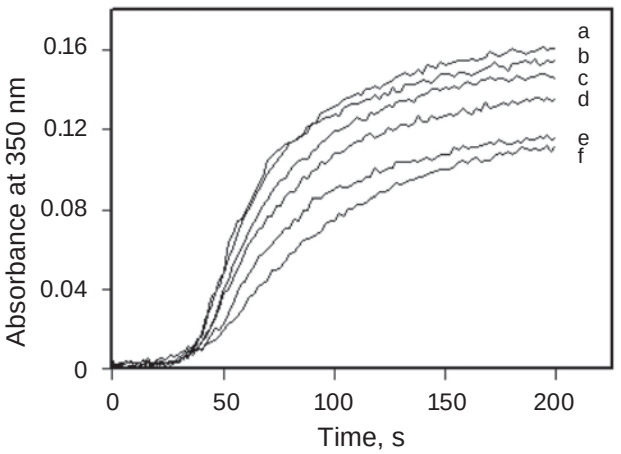

Fig. 5. Turbidity analysis of inhibition of fibrin desAB polymerization by the synthetic peptide Bβ125-135 and its scrambled version. Curves: ***a****, fibrin desAB polymerization (100 μg/ml) without peptides,* ***b****, fibrin desAB polymerization with scrambled peptide (0.5 mM), and fibrin desAB polymerization with* ***c****, 0.125 mM peptide,* ***d****, 0.25 mM peptide,* ***e****, 0.375 mM peptide, and* ***f****, 0.5 mM peptide. Each curve is an average of 2 repeats*

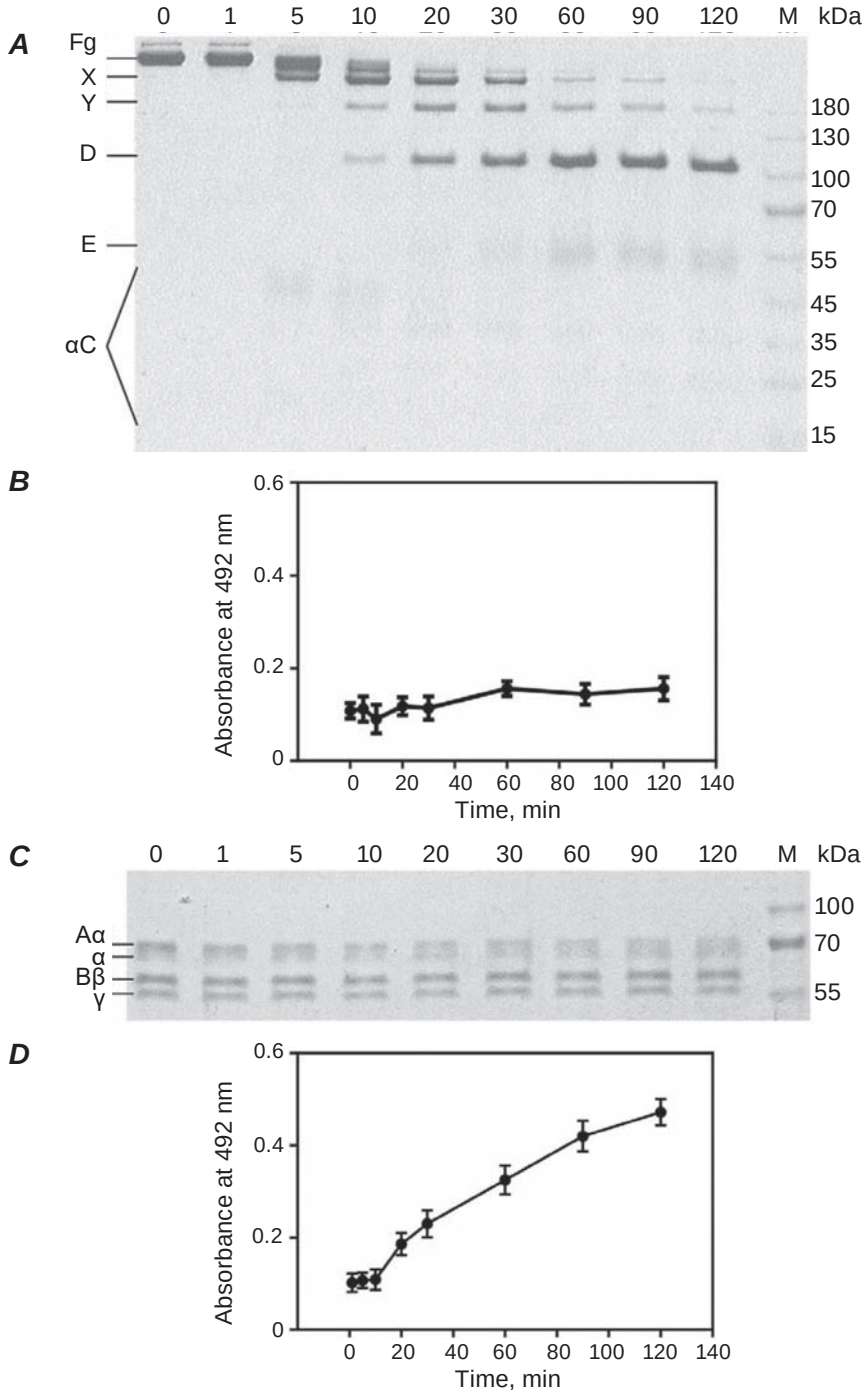

*Fig. 6. Exposure of mAb FnI-3c epitope during hydrolysis of fibrinogen by plasmin and thrombin. Fibrinogen was added at the concentration of 0.2 mg/ml to the medium, containing 0.02 M HEPES buffer pH 7.4, 0.3 M NaCl, and the reaction was initiated by plasmin or thrombin/Reptilase at 0.005 NIH/ml. At a given time, the reaction was stopped by adding PMSF and aprotinin to final concentrations of 1 mM and 10 mkg/ml, respectively. Aliquots were withdrawn for electrophoretic and ELISA analysis. Aliquots for ELISA were added to microtitre plate wells. Neoantigenic determinant exposure was analyzed with mAb FnI-3c as the primary- and sheep anti-mouse IgG-HRP conjugate as the secondary antibodies. Samples of mediums of the (**A**, **B**) fibrinogen-plasmin and (**C**, **D**) fibrinogen-thrombin/Reptilase reactions were subjected to electrophoresis (**A**, **C**) and ELISA (**B**, **D**). Data represent 3 independent experiments. Error bars represent the standard deviations of the mean values*

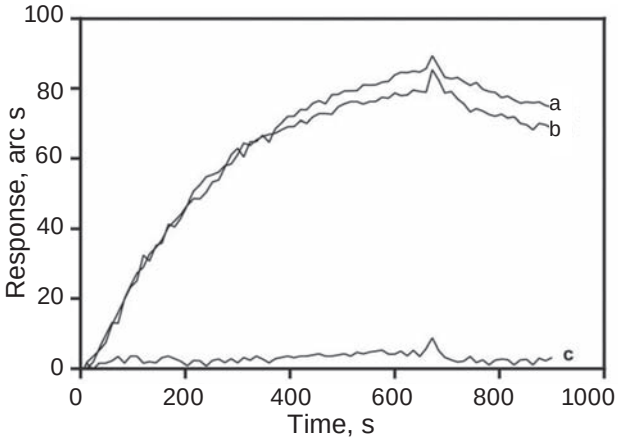

Fig. 7. Binding of fibrin desA formed in situ to mAb FnI-3c in the presence and absence of the GPRP peptide as detected by the SPR method. Fibrin-specific mAb FnI-3c was immobilized into working and control cells of a biosensor chamber. Fibrinogen was added to the control cell at 1 μg/ml concentration in 0.02 M HEPES buffer, pH 7.4, 0.3 M NaCl, with 0.005% of Tween-20. In the working cell, fibrinogen was added to the same medium with the addition of 0.001 NIH units/ml of Reptilase in the presence or absence of 1 mM GPRP peptide. The interaction between fibrin desA, formed in situ, and the mAb immobilized on the chip was registered by the SPR method. The curves of the difference between signals from working and control cells are presented. Curves: ***a****, fibrinogen + Reptilase;* ***b****, fibrinogen + Reptilase + GPRP; and c, fibrinogen as a control. Each curve represent an average of 3 repeats*

more exposed in fibrin. During the fibrinogen to fibrin transformation, the surface of the Bβ125-135 site flattens due to the emergence of the α-helical fragment partially buried in fibrinogen (Fig. 8, *B, C, D*).

The mAb FnI-3c and its Fab-fragment inhibit the lateral association of protofibrils in the process of fibrin polymerization [8]. We showed that synthetic peptides imitating the amino acid sequence of fibrin/fibrinogen fragments Bβ121-138 and Bβ125-135 also inhibit this stage of fibrin polymerization. Initially, we supposed that the fragment Bβ125-135 was the contact site of the inter-protofibril lateral binding. However, several facts now indicate that this site of the coiled-coil adopts a structure important for the subsequent association of fibrin protofibrils, and that the epitope exposure in Bβ125-135 reflects this structural rearrangement. In this regard, there are known mutations in the α-, β-, and γ-constituents

Table. Per-residue surface area of the exposed residues of Bβ126-139 fragment of fibrinogen (S_{Fg}) and fibrin (S_{Fn}). The surface area changes (S_{Fn}–S_{Fg}) in the models obtained by conformational analysis were calculated

Residue	S_{Fg} (Å^2)	S_{Fn} (Å^2)	ΔS (S_{Fn}–S_{Fg}) (Å^2)
BβQ126	107.1	108.0	0.9
BβK127	117.1	107.3	-9.7
BβR128	141.8	144.9	3.1
BβK130	117.7	119.1	1.4
BβQ131	109.8	111.4	1.6
BβK133	118.8	115.7	-3.1
BβD134	88.4	95.0	6.6
BβN135	87.6	98.4	10.8
BβN137	99.8	104.2	4.4
BβV138	89.8	95.1	5.3
BβV139	91.9	97.0	5.1

of the coiled-coil containing Bβ111-141 that impair fibrin polymerization [31-36]. Moreover, our structural biological analysis of the Bβ125-135 site showed that conformational rearrangements take place in the hinge region during the fibrinogen-fibrin transition with the accompanying formation of the neoantigenic determinant which is preserved in the subsequent stages of fibrin polymerization.

We propose that at the start of protofibril lateral association, a specific bend and/or twist in two coiled-coil hinge regions of the dimeric fibrin molecule is required. This structural rearrangement provides a necessary mutual spatial orientation of the other regions of the molecule, which come into direct inter-protofibril contact during protofibril lateral association [6]. Our data show that the cleavage of Fp A during the fibrinogen-fibrin conversion induces the intramolecular structural rearrangement within the monomeric molecule of fibrin desA, and increases the flexibility in hinge regions. These structural changes are necessary for the subsequent protofibril association stage.

The augmentation of the flexibility in the hinge fragments of fibrin causes the increase of bending and twisting motions in the coiled-coil connector as compared to fibrinogen. Any factor affecting the flexibility of fibrin molecules in the hinge region will impair protofibril lateral association. The binding of the mAb FnI-3c or Fab-fragment to their epitope in

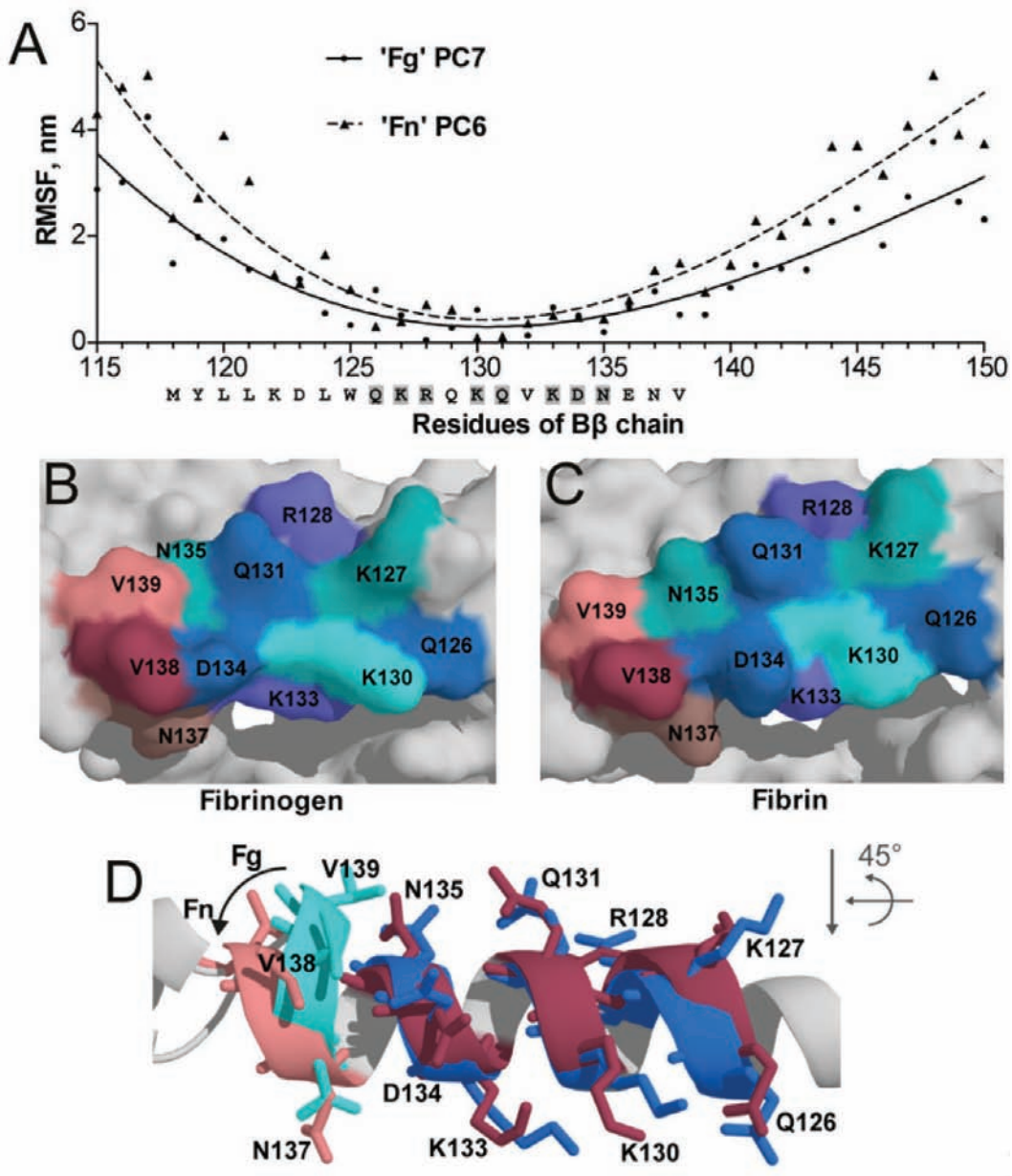

*Fig. 8. Comparative RMSF analysis of conformational changes into hinge loci of fibrinogen and fibrin fragments X. (**A**) RMSF of the Bβ115-150 fragment C-alpha atoms for the principal component 7 for fibrinogen ('Fg' PC7, ●) and for the principal component 6 for fibrin ('Fn' PC6, ▲) ensembles of the conformations. Solid and dashed lines represent cubic polynomial approximations of the RMSF data for fibrinogen and fibrin, respectively. The coefficient of determination (R^2) is 0.87 and 0.81 for fibrinogen and fibrin, respectively. The amino acid residues of fragment Bβ118-138 are denoted. The residues postulated to form the epitope for fibrin-specific mAb FnI-3c are marked with grey boxes. (**B**, **C**) Surface formed by the amino acid residues of fragment Bβ126-139 in models of (**B**) fibrinogen and (**C**) fibrin obtained by conformational analysis. (**D**) Structurally superimposed alpha-helical fragments Bβ126-139 from the selected models of fibrinogen and fibrin obtained by conformational analysis. The view in (**D**) is rotated by 45° around the long axis of the molecule compared to the views in (**B**) and (**C**). The residues Bβ Q126, K127, R128, K130, Q131, K133, D134, and N135 of fibrinogen and fibrin are assumed to form the epitope for mAb FnI-3c. Residues Bβ N137, V138, and V139 shield the residues Bβ D134 and N135 in fibrinogen. The latter become more exposed in fibrin*

the hinge region inhibited the polymerization process. The impairment of fibrin polymerization by the synthetic peptides Bβ121-138 and Bβ125-135 may be caused by decreased flexibility at the hinge loci of separate fibrin molecules in forming protofibrils. These peptides may bind with the corresponding α- or γ-remnants of the hinge region in the fibrin coiled-coil and block the bending motions. This mechanism may be similar to the self-assembly of the coiled-coil from peptides described by Jing et al. for the synthetic peptides imitating the human fibrinogen site γ23-57 and its modified form [37].

Conclusions

Cleavage of fibrinopeptide A exposes a stable neoantigenic determinant in the fibrin desA Bβ125-135 site. Bβ125-135 is a constituent of the fibrin hinge consisting of Aα91-103, Bβ125-135, and γ69-77. The flexibility of the hinge is increased during the fibrinogen to fibrin transformation. We assume the increase in flexibility in the fibrin molecule around the hinges allows the structural reorganization of the fibrin desA molecule during the self-assembling of protofibrils and their lateral association into fibrils.

Conflict of interest. Authors have completed the Unified Conflicts of Interest form at http://ukrbiochemjournal.org/wp-content/uploads/2018/12/coi_disclosure.pdf and declare no conflict of interest.

Funding sources. The study was supported by the Project № 0114U003217 (01/2014-12/2018) "The study of the mechanism of the fibrin framework of thrombus formation and the development of test-systems for the diagnostics of hemostasis inflammation processes, cardiovascular diseases and surgery."

Acknowledgements. We thank Cedars-Sinai Medical Center's International Research and Innovation in Medicine Program and the Association for Regional Cooperation in the Fields of Health, Science and Technology (RECOOP HST) Association for their support of our organization as a participating Cedars-Sinai Medical Center – RECOOP Research Center (CRRC).

Bβ125-135 ДІЛЯНКА МОЛЕКУЛИ ФІБРИНУ БЕРЕ УЧАСТЬ У ЛАТЕРАЛЬНІЙ АСОЦІАЦІЇ ПРОТОФІБРИЛ

Е. Луговською[1], *М. Пидюра*[2], *Є. Макогоненко*[1]✉, *Л. Урвант*[1], *П. Гриценко*[1], *І. Колеснікова*[1], *Н. Луговська*[1], *С. Комісаренко*[1]

[1]Інститут біохімії ім. О. В. Палладіна НАН України, Київ;
[2]Інститут харчової біотехнології та геноміки НАН України, Київ;
✉e-mail: ymakogonenko@gmail.com

Раніше ми показали, що в процесі перетворення фібриногену людини у фібрин на фрагменті Bβ119-133, який розташований у шарнірний ділянці молекули, експонується неоантигенна детермінанта. Фібринспецифічне mAb FnI-3c та його Fab-фрагмент, епітоп для яких знаходиться в цьому фрагменті, гальмують латеральну асоціацію протофібрил. Ми припустили, що епітоп співпадає із сайтом, який бере участь у цьому процесі. У цій роботі ми більш точно визначили розташування епітопу для mAb FnI-3c у молекулі фібрину та встановили його роль у функціонуванні шарнірного локусу молекули. Було виявлено, що mAb FnI-3c зв'язується з фібрином людини, коня та кроля, які мають лізин у положенні, що відповідає такому BβK130 фібрину людини, але відсутній у фібрині бика та щура, у яких в цьому положенні є інші амінокислотні залишки, що вказує на те, що залишок BβK130 є невід'ємною складовою епітопу. Цей факт, дані гомології та структурно-біологічний аналіз амінокислотних послідовностей навколо BβK130 свідчать про те, що досліджуваний сайт локалізований у межах Bβ125-135 молекули фібрину. Синтетичні пептиди Bβ125-135 та Bβ121-138, на відміну від їхніх неупорядкованих аналогів, зв'язуються з FnI-3c в ППР аналізі. Обидва пептиди на відміну від їхніх неупорядкованих версій, інгібували латеральну асоціацію протофібрил. Епітоп

mAb FnI-3c експонується після відщеплення фібринопептиду А та утворення мономеру desA фібрину. Структурний біологічний аналіз переходу фібриногену у фібрин показав чітке підвищення рухливості в шарнірному локусі. Ми вважаємо, що така структурна перебудова в шарнірних областях фібрину спричинює формування конформації молекули, яка необхідна для латеральної асоціації протофібрил фібрину.

Ключові слова: трансформація фібриногену у фібрин, суперспіралізований конектор, латеральна асоціація протофібрил, шарнірна ділянка, неоантигенна детермінанта.

References

1. Medved L, Weisel JW. Recommendations for nomenclature on fibrinogen and fibrin. *J Thromb Haemost.* 2009; 7(2): 355-359.
2. Doolittle RF, Goldbaum DM, Doolittle LR. Designation of sequences involved in the "coiled-coil" interdomainal connections in fibrinogen: constructions of an atomic scale model. *J Mol Biol*. 1978; 120(2): 311-325.
3. Köhler S, Schmid F, Settanni G. The Internal Dynamics of Fibrinogen and Its Implications for Coagulation and Adsorption. *PLoS Comput Biol*. 2015; 11(9): e1004346.
4. Lugovskoy EV, Gritsenko PG, Kapustianenko LG, Kolesnikova IN, Chernishov VI, Komisarenko SV. Functional role of Bbeta-chain N-terminal fragment in the fibrin polymerization process. *FEBS J*. 2007; 274(17): 4540-4549.
5. Yang Z, Mochalkin I, Doolittle RF. A model of fibrin formation based on crystal structures of fibrinogen and fibrin fragments complexed with synthetic peptides. *Proc Natl Acad Sci USA*. 2000; 97(26): 14156-14161.
6. Kollman JM, Pandi L, Sawaya MR, Riley M, Doolittle RF. Crystal structure of human fibrinogen. *Biochemistry*. 2009; 48(18): 3877-3886.
7. Hanss M, Biot F. A database for human fibrinogen variants. *Ann N Y Acad Sci*. 2001; 936: 89-90.
8. Lugovskoy EV, Gritsenko PG, Kolesnikova IN, Lugovskaya NE, Komisarenko SV. A neoantigenic determinant in coiled coil region of human fibrin beta-chain. *Thromb Res.* 2009; 123(5): 765-770.
9. Brown JH, Volkmann N, Jun G, Henschen-Edman AH, Cohen C. The crystal structure of modified bovine fibrinogen. *Proc Natl Acad Sci USA*. 2000; 97(1): 85-90.
10. Varetskaya TV. Microheterogeneity of fibrinogen. Cryofibrinogen. *Ukr Biokhim Zhurn*. 1960; 32(1): 13-27.
11. Belitser VA, Varetskaja TV, Malneva GV. Fibrinogen-fibrin interaction. *Biochim Biophys Acta*. 1968; 154(2): 367-375.
12. Lougovskoi EV, Gogolinskaya GK. Preparation of fibrin des-AA by thrombin. *Ukr Biokhim Zhurn*. 1999; 71(4): 107-108.
13. Fenton JW 2nd, Fasco MJ, Stackrow AB. Human thrombins. Production, evaluation, and properties of alpha-thrombin. *J Biol Chem.* 1977; 252(11): 3587-3598.
14. Deutsch DG, Mertz ET. Plasminogen: purification from human plasma by affinity chromatography. *Science*. 1970; 170(3962): 1095-1096.
15. Robbins KC, Summaria L. Plasminogen and plasmin. *Methods Enzymol*. 1976; 45: 257-273.
16. Köhler G, Milstein C. Continuous cultures of fused cells secreting antibody of predefined specificity. *Nature*. 1975; 256(5517): 495-497.
17. Lugovskoi EV, Makogonenko EM, Chudnovets VS, Derzskaya SG, Gogolinskaya GK, Kolesnikova IN, Bukhanevich AM, Sitak IN, Lyashko ED, Komisarenko SV. The study of fibrin polymerization with monoclonal antibodies. *Biomed Sci*. 1991; 2(3): 249-256.
18. Li XM, Huskens J, Reinhoudt DN. Reactive self-assembled monolayers on flat and nanoparticle surfaces, and their application in soft and scanning probe lithographic nanjfabrication technologies. *J Mater Chem.* 2004; 14(20): 2954-2971.
19. Laemmli UK. Cleavage of structural proteins during the assembly of the head of bacteriophage T4. *Nature*. 1970; 227(5259): 680-685.
20. Mills D, Karpatkin S. The initial macromolecular derivatives of human fibrinogen produced by plasmin. *Biochim Biophys Acta*. 1972; 271(1): 163-173.
21. Eswar N, Webb B, Marti-Renom MA, Madhusudhan MS, Eramian D, Shen MY, Pieper U, Sali A. Comparative protein structure modelling using Modeller. *Curr Protoc Bioinformatics*. 2006; 15(1): 5.6.1-5.6.30.
22. Martí-Renom MA, Stuart AC, Fiser A, Sánchez R, Melo F, Sali A. Comparative protein structure modeling of genes and genomes. *Annu Rev Biophys Biomol Struct*. 2000; 29: 291-325.

23. Sali A, Blundell TL. Comparative protein modelling by satisfaction of spatial restraints. *J Mol Biol*. 1993; 234(3): 779-815.
24. Fiser A, Do RK, Sali A. Modeling of loops in protein structures. *Protein Sci*. 2000; 9(9): 1753-1773.
25. Chen VB, Arendall WB 3rd, Headd JJ, Keedy DA, Immormino RM, Kapral GJ, Murray LW, Richardson JS, Richardson DC. MolProbity: all-atom structure validation for macromolecular crystallography. *Acta Crystallogr D Biol Crystallog.* 2010; 66(Pt 1): 12-21.
26. de Groot BL, van Aalten DM, Scheek RM, Amadei A, Vriend G, Berendsen HJ. Prediction of protein conformational freedom from distance constraints. *Proteins.* 1997; 29(2): 240-251.
27. Bakan A, Meireles LM, Bahar I. ProDy: protein dynamics inferred from theory and experiments. *Bioinformatics.* 2011; 27(11): 1575-1577.
28. Humphrey W, Dalke A, Schulten K. VMD: visual molecular dynamics. *J Mol Graph.* 1996; 14(1): 33-38.
29. DeLano WL. The PyMOL Molecular Graphics System. DeLano Scientific, San Carlos, CA 2002.
30. Abyzov A, Bjornson R, Felipe M, Gerstein M. RigidFinder: a fast and sensitive method to detect rigid blocks in large macromolecular complexes. *Proteins.* 2010; 78(2): 309-324.
31. Keating KS, Flores SC, Gerstein MB, Kuhn LA. StoneHinge: hinge prediction by network analysis of individual protein structures. *Protein Sci.* 2009; 18(2): 359-371.
32. Okumura N, Terasawa F, Hirota-Kawadobora M, Yamauchi K, Nakanishi K, Shiga S, Ichiyama S, Saito M, Kawai M, Nakahata T. A novel variant fibrinogen, deletion of Bbeta111Ser in coiled-coil region, affecting fibrin lateral aggregation. *Clin Chim Acta.* 2006; 365(1-2): 160-167.
33. Hanss M, Ffrench P, Vinciguerra C, Bertrand M-A, Mazancourt P. Four cases of hypofibrinogenemia associated with four novel mutations. *J Thromb Haemost.* 2005; 3(10): 2347-2349.
34. Brennan SO, Davis RL, Lowen R, Ruskova A. Deletion of five residues from the coiled coil of fibrinogen (Bbeta Asn167_Glu171del) associated with bleeding and hypodysfibrinogenemia. *Haematologica.* 2009; 94(4): 585-588.
35. Kotlín R, Reicheltová Z, Malý M, Suttnar J, Sobotková A, Salaj P, Hirmerová J, Riedel T, Dyr JE. Two cases of congenital dysfibrinogenemia associated with thrombosis-Fibrinogen Praha III and Fibrinogen Plzen. *Thromb Haemost.* 2009; 102(3): 479-486.
36. Marchi RC, Meyer MH, de Bosch NB, Arocha-Piñango CL, Weisel JW. A novel mutation (deletion of Aalpha-Asn 80) in an abnormal fibrinogen: fibrinogen Caracas VI. Consequences of disruption of the coiled coil for the polymerization of fibrin: peculiar clot structure and diminished stiffness of the clot. *Blood Coagul Fibrinolysis.* 2004; 15(7): 559-567.
37. Jing P, Rudra JS, Herr AB, Collier JH. Self-assembling peptide-polymer hydrogels designed from the coiled coil region of fibrin. *Biomacromolecules.* 2008; 9(9): 2438-2446.